WORLD CONFERENCE ON TIMBER ENGINEERING 2025
BRISBANE, AUSTRALIA
Advancing Timber for the Future Built Environment

DEVELOPMENT OF GIR SYSTEM IMPROVED ON-SITE WORKABILITY

Y.Mori[1], K.Nagai[2], T.Kayukawa[3], K.Tanaka[4], H.Yamane[5], Y.Kawano[6]

ABSTRACT: In this study develops a connection system using connectors that improve deformation performance, and conducts structural experiments assuming the connections of a 3-4 story wooden frame building, along with performance evaluation. In all specimens, the Structural Characteristic Coefficient was below 0.5, showed high performance. Additionally, a full-scale lateral loading experiment was conducted. Moving forward, a detailed examination will be conducted regarding the consistency between the results of the connection experiments and the full-scale frame tests using this connection system.

KEYWORDS: GIR system, toughness connectors, box-shaped metal bracket

1 – INTRODUCTION

In recent years, building standards had revised to promote wooden large-scale or mid-rise buildings in Japan. It is expected that the number of medium- to large-scale wooden buildings will increase in the future. The realization of these buildings requires higher structural performance than conventional wooden building techniques. This situation has increased the demand for timber building and the use of moment-resisting frame structures, which can achieve the same floor plans as buildings of steel or RC construction. The structural performance of a moment resisting frame structure is largely dependent on the stiffness and strength of the joints. For this reason, the GIR joint system, which combines high strength and high rigidity, is attracting attention. The typical GIR joint system faces issues with deformation capacity and toughness due to the potential for brittle fracture. Against this background, our research laboratory has conducted structural experiments aimed at clarifying the performance of moment-resisting connections using connectors (referred to as "toughness connectors") that control the yield strength and yield position, applied to the column-beam connections of a mid-scale wooden frame building. The goal of these experiments has been to understand the performance of these connections. [1] This toughness connector consists of a single rod with a smooth section for yielding and deformation, and threaded sections at both ends for adhesive bonding.

The frame part of the medium-scale wooden frame structure building is shown in Fig. 1.

This study aimed to organize structural design data through the implementation of structural experiments considering column bases joint, Exterior Beam-Column joint, Plus-shaped joints, L-shaped joints, and T-shaped joints, as well as the evaluation of their structural performance and the establishment of a design method for this connection system.

Furthermore, to verify the applicability of the previous connection experiments to the behavior of full-scale frames, a full-scale lateral loading experiment was conducted on the lower two-story portion of a mid-scale wooden frame building.

1 Yuta Mori, Oita Univ., Oita, Japan, v2157445@oita-u.ac.jp

2 Kota Nagai, Oita Univ., Oita, Japan, v2157432@oita-u.ac.jp

3 Takato Kayukawa, Oita Univ., Oita, Japan, v24e5003@oita-u.ac.jp

4 Kei Tanaka, Oita Univ., Oita, Japan, kei@oita-u.ac.jp

5 Hikaru Yamane, Ebisu Architectural Institute Co., Tokyo, Japan, yamane@ebi-ken.co.jp

6 Yasuyuki Kawano, SCRIMTEC JAPAN Co., Fukuoka, Japan, kawano@scrimtec.co.jp

https://doi.org/10.52202/080513-0019

2 – EXPERIMENTAL OVERVIEW

2.1 Test Specimens

Table 1 presents the list of test specimens, Fig. 2 shows the shape of the toughness connector, Fig. 3 illustrates the detail of column-beam joint using the GIR system, and Fig. 4 to 8 shows the shapes and sizes of the various connection test specimens. Photo 1 display the Buckling-resistant steel tube. In a typical GIR joint system, the timber is joined by injecting adhesive at the construction site. This type of work is disliked by builders because it requires temporary supports and working space while the adhesive cures. Therefore, by inserting a box-shaped metal connector between the components, an improved GIR connection method was developed, combining the high connection performance of GIR with the constructability of bolt connections. This connection method involves adhesive injection at the laminated timber factory, and only bolt tightening is required at the construction site. The toughness rod used in this system consists of an M30 fully threaded bolt as fixing part and an M20 round steel bar as toughness part (see Fig. 2). In the previous research, wood splitting failure occurred due to the buckling of toughness connectors (see Photo.1). To prevent this, a steel tube was reinforced around the toughness part.

The laminated timber used as all test specimens is made of larch and meets the strength standard JAS: E95-F270. The JAS standards are regulations that define the quality criteria for wood products and other materials in Japan.

Two toughness rods were inserted into each end of the column base joint. Beams of exterior Beam -column joint and L-shape joint have two toughness rods inserted at both ends of the beam depth. Additionally, for T-shape joints and Plus-shape joints, one toughness rods is inserted on each side. On the other hand, one full-threaded bolt (M30: equivalent to JIS S45C) was fixed to the column with adhesive, on each side, according to the size of the beam to which it was attached. Each joint is fastened on the construction site by a high-strength bolt between box-shaped metal bracket fitting attached to the beam by toughness GIR and high-strength nut attached to fully threaded bolt in the column. These high-strength bolts were torqued to 100Nm. Shear brackets were installed to prevent the GIR from bearing the shear force. These shear brackets are made of T-shaped steel member and are attached to each member with some small GIR. T-shape steel members with long holes to prevent the transfer of tensile loads, are fastened together with two gusset plates and bolts. These high-strength bolts were torqued to 100Nm.

The adhesive used in the GIR joints is epoxy resin adhesive and curing period of adhesive is 7 days.

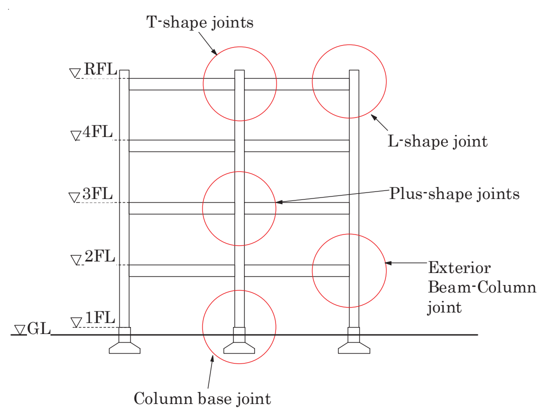

Fig.1 The frame part of the medium-scale wooden frame structure building

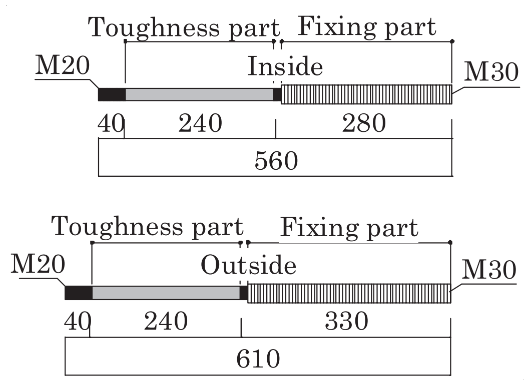

Fig.2 Detail of Toughness rod

Table 1: The list of test specimens

Specimen shape	Column base	Exterior Beam-Column joint	Plus-shape	T-shape	L-shape
Specimen name	C12CS3	E12GS3	P12GS3	T12GS3	L12GS3
Wood species	Larch(JAS:E95-F270)				
Cross-section of column (mm)	120×600	120×600	120×600	120×600	120×600
Cross-section of beam (mm)		120×600	120×600	120×600	120×600
Number of specimens	3	3	2	3	3

https://doi.org/10.52202/080513-0019

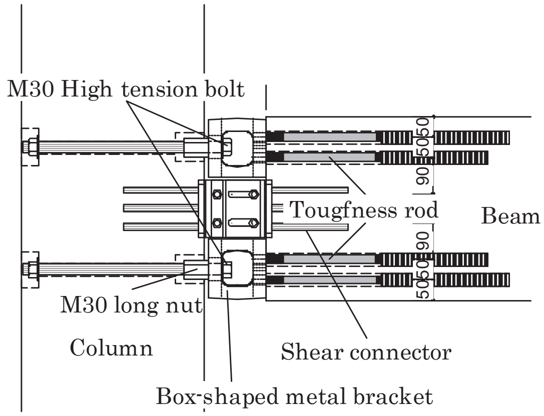

Fig.3 Detail of column-beam joint using the GIR system

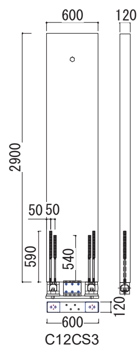

Fig. 4 Size and shape of Specimen (mm) - Column Base joint

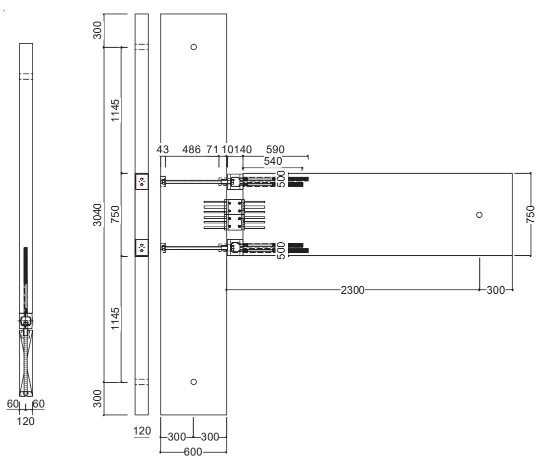

Fig. 5 Size and shape of Specimen (mm) Exterior Beam-Column joint

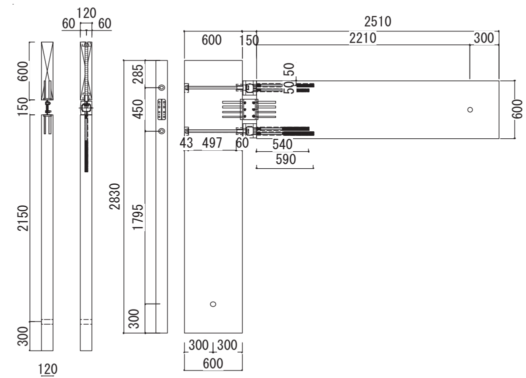

Fig. 6 Size and shape of Specimen (mm) – L-shape joint

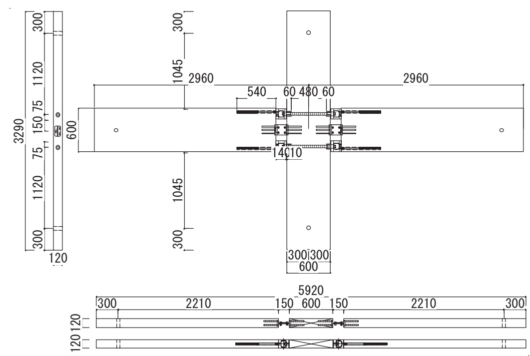

Fig. 7 Size and shape of Specimen (mm) – Plus-shape joints

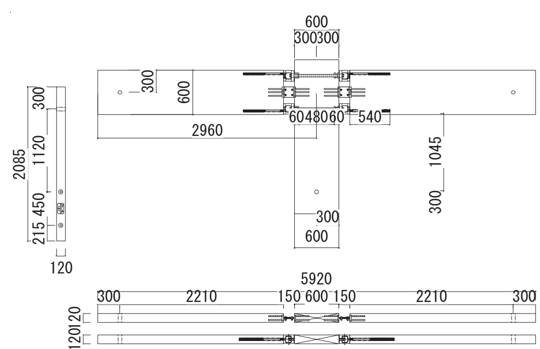

Fig. 8 Size and shape of Specimen (mm) – T-shape joints

Photo 1 Buckling-resistant steel tube

2.2 Method of joint test

Fig. 9 to 13 shows the Test set-up for joint test. The loading tests are carried out according to the rule specified by the testing manual of Japanese standard [2]. The cyclic loading protocol consist of deformations to give apparent deformation angles of 1/450, 1/300, 1/200, 1/150, 1/100, 1/75 , 1/50 and 1/30 radians. In each cyclical loop, 3 cycles loading is applied. Subsequently, the loading was increased up to 1/15 rad. The pulling direction of the jack is considered the positive loading direction, and the pushing direction is considered the negative loading direction. The loading was applied using a 500 kN double-acting hydraulic jack (Riken Seiki Co., Ltd.: D5-500).

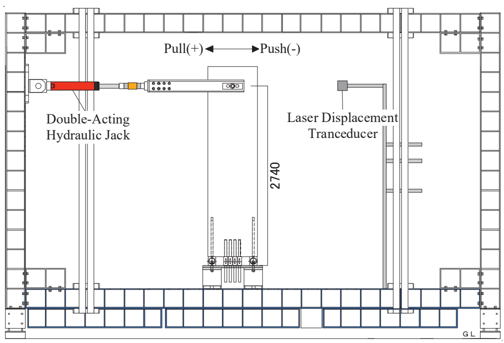

Fig. 9 Test set up (mm) - Column Base joint

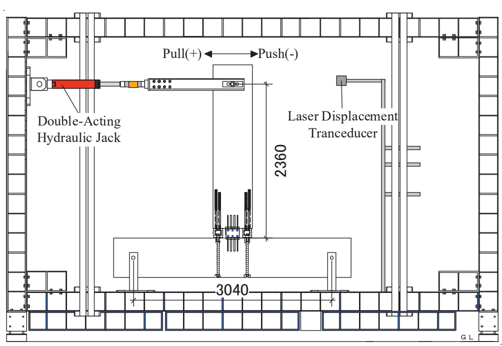

Fig. 10 Test set up (mm) - Exterior Beam-Column joint

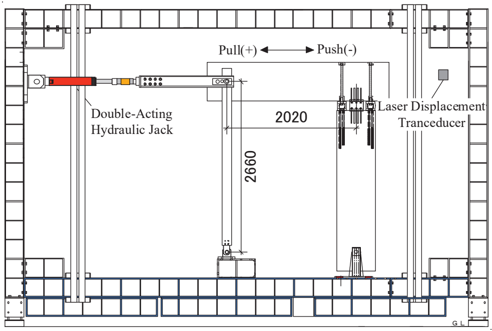

Fig. 11 Test set up (mm) - L-shape joint

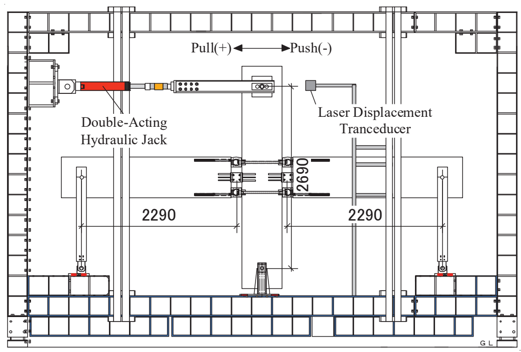

Fig. 12 Test set up (mm) - Plus-shape joints

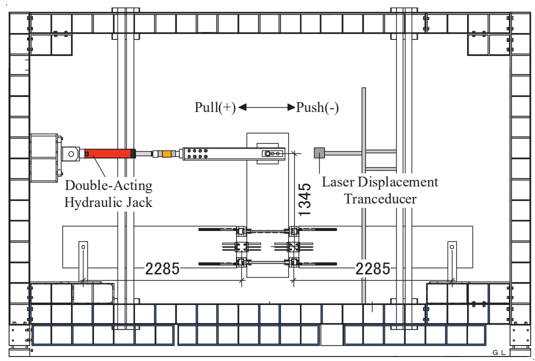

Fig. 13 Test set up (mm) - T-shape joints

3 – TEST RESULTS

3.1 Evaluation Method

The derivation of the moment-connection deformation angle relationship (hereinafter referred to as the M-θ relationship) was conducted in the same manner as in previous studies [3].

3.2 Moment-Deformation Angle Relationship

Fig. 14 to 18 shows the typical relationships between bending moment and deformation angle of connection. Photos 2 to 6 display the representative failure modes.

The moment-deformation angle relationship is considered for each joint of the T-shape and Plus-shape joints. The specimens of C12CS3 maintained high stiffness up to 1/100 rad and exhibited yielding behavior at 1/75 rad. No cracking was observed thereafter, and the load increased until reaching 1/15 rad (see Photo 1). In the E12GS3 series, all specimens exhibited yielding behavior at 1/50 rad. Afterward, shear failure occurred in the panel zone of the column during loading at 1/15 rad, leading to a decrease in load (see Photo 2). In the L12GS3 series, all specimens exhibited yielding behavior at 1/30 rad. Subsequently, during loading at 1/15 rad, bending

https://doi.org/10.52202/080513-0019

failure of the column occurred at the GIR rod location on the tensile side of the column (see Photo 3). In the P12GS3 series, all specimens exhibited yielding behavior at 1/50 rad. Subsequently, during loading at 1/15 rad, shear failure occurred in the panel zone (see Photo 4). In the T12GS3 series, all specimens exhibited yielding behavior at 1/50 rad. Subsequently, during the first positive loading at 1/30 rad, shear failure occurred in the panel zone of the column. Later, during loading at 1/15 rad, bending failure of the column occurred at the GIR rod location on the tensile side of the column (see Photo 5).

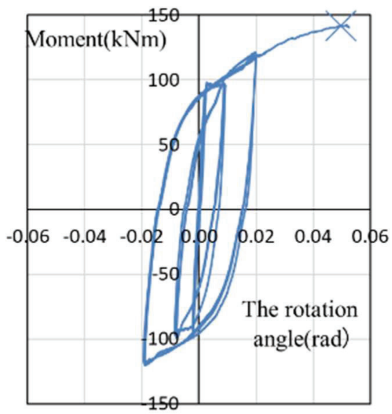

Fig. 14 M- θ relationship C12CS3 No.1

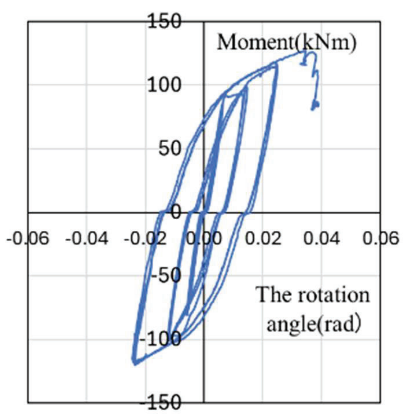

Fig. 15 M- θ relationship E12GS3 No.1

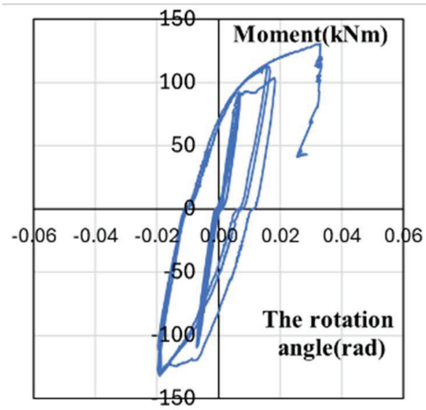

Fig. 16 M- θ relationship L12GS3 No.1

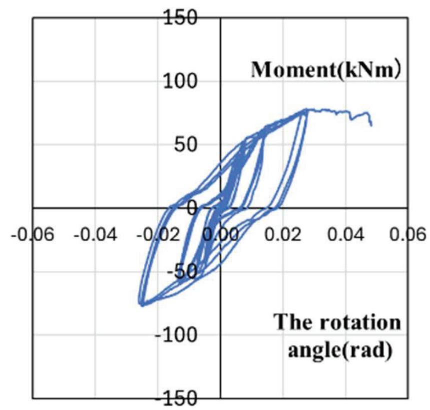

Fig. 17 M- θ relationship P12GS3 No.1

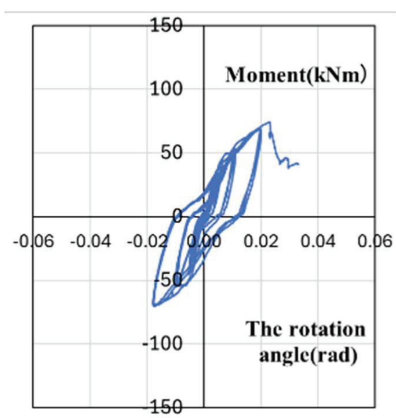

Fig. 18 M- θ relationship T12GS3 No.1

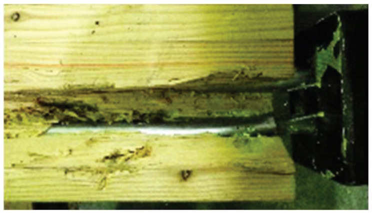

Photo 2 Failure modes C12GS3 No.1
buckling of the toughness connector

Photo 3 Failure modes E12GS3 No.1
Destruction in the panel zone

Photo 4 Failure modes L12GS3 No.1
Bending failure of a column

Photo 5 Failure modes P12GS3 No.1
Destruction in the panel zone

Photo 6 Failure modes T12GS3 No.1
Destruction in the panel zone

3.3 Rotational Stiffness

The rotation stiffness is shown in Fig. 19. When comparing specimens with the same number of connectors, the rotation stiffness of L12GS3 is approximately 1.1 times greater than that of E12GS3, while the rotation stiffness of T12GS3 is about 1.2 times greater than that of P12GS3.

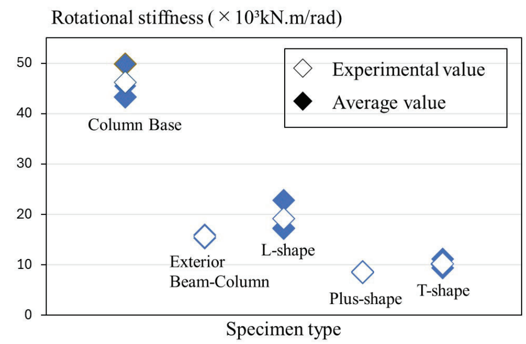

Fig. 19 Rotational stiffness

3.4 Yield moment and Maximum moment

Fig. 20 shows the yield moment and maximum moment. Regarding yield strength, when comparing specimens with the same number of connectors, L12GS3 and E12GS3 exhibit similar values for yield strength, while P12GS3 shows a value approximately 1.2 times higher than that of T12GS3. The maximum strength of T12GS3 is approximately 1.1 times greater than that of L12GS3, and J12GS3 is about 1.1 times higher than T12GS3. Regarding the variation in the maximum strength, the cause in all specimens is attributed to the failure of the timber at ultimate failure.

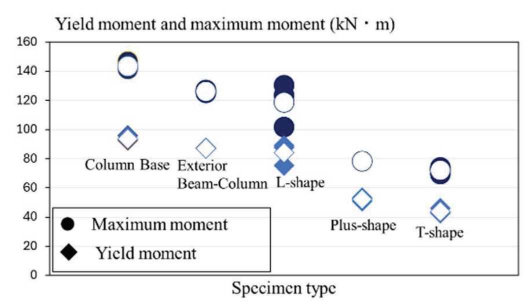

Fig.20 Yield moment and Maximum moment

3.5 Structural characteristic coefficient

Fig. 21 shows the Structural Characteristic Coefficient. The Structural Characteristic Coefficient is a coefficient that evaluates the energy absorption capacity associated

https://doi.org/10.52202/080513-0019

with plastic deformation capacity and damping characteristics.

Plasticity Ratio μ: It is the ratio of the displacement δu at yield to the displacement δv at ultimate failure.

$$\mu = \frac{\delta u}{\delta v}$$

Structural Characteristic Coefficients Ds: More ductile structures exhibit smaller values.

$$Ds = \frac{1}{\sqrt{2\mu - 1}}$$

In all specimens, the Structural Characteristic Coefficient, was below 0.5. It was demonstrated that higher deformation performance compared to moment-resisting connections using existing GIR system.

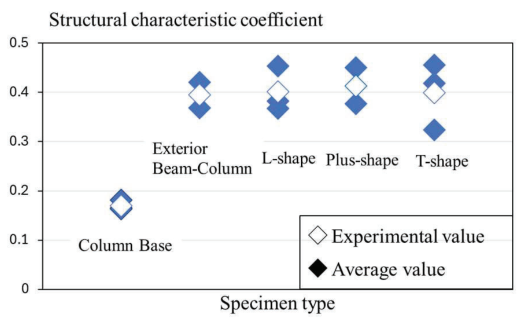

Fig. 21 Structural characteristic coefficient

4 – A FULL-SCALE FRAME LATERAL FORCE TEST

Full-scale lateral load tests were carried out, assuming the lower two story of a four-story wooden building.

4.1 Test Specimen

The shape of the test specimen is shown on Fig. 22. The laminated timber used as all test specimens is made of Sugi and meets the strength standard JAS: E95-F270. The columns will have a cross-section of 105×600 mm, while the second and third-floor beams will have a cross-section of 105×750 mm. The floor height will be 3200 mm on the first floor and 3275 mm on the second floor. The joint method at the column-beam joints will be the same as the Exterior Beam-Column specimen described in Chapter 2. The column base joint will also be the same as described in Chapter 2.

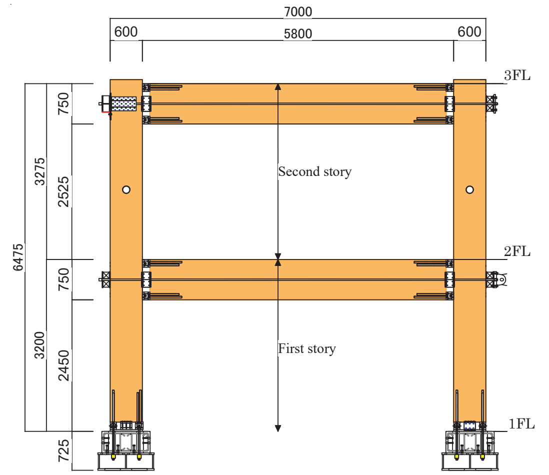

Fig. 22 The size and shape of the test specimen of full-scale

4.2 Test Method of Full-Scale Frame Test

Fig. 23 shows the Test sets-up for Full-Scale Frame. The vertical load on the specimen was calculated from an assumed four-story building. The vertical loads on the third story and fourth story, were split in two and placed on two columns. The second floor load was loaded at one point, and the third floor load was loaded at two points by applying weights at locations where the moment distribution was equivalent to the equally distributed load of the floor load. The horizontal load is applied by clamping the beams of the specimen with a fixture and securing them with a PC steel rod. The load is then applied using a hydraulic jack from the reaction wall.

The cyclic loading protocol consists of deformations to give apparent deformation angles of 1/450, 1/300, 1/200, 1/150, 1/100, 1/75, and 1/50 radians. In each cyclical loop, 3 cycles loading is applied. 1/30 cyclical loop, 1 cycle loading is applied. Subsequently, the loading was increased up to 1/15 rad.

The experiment was carried out under load control until yielding. After yielding, the control method was changed to displacement control.

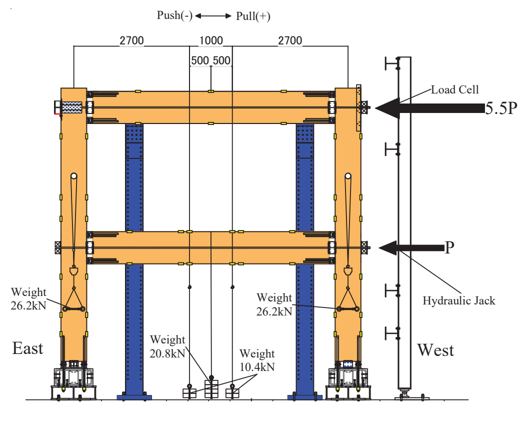

Fig. 23 Test sets up of Full-Scale Frame

5 – TEST RESULTS

5.1 Lateral Force- Story Deformation Angle

The relationship between the lateral force of each story and the story deformation angle for the first and second storys is shown in Fig. 24 and 25. Photos 7 and 8 display the main failure modes. Up to the loading of 1/100 rad, the load-deformation relationship for each story exhibited high stiffness. In the loading of 1/75 rad, yielding behavior began to emerge during positive loading. In the loading of 1/50 rad, yielding behavior was observed during one cycle of negative loading.

In the loading of 1/30 rad, the positive side shear force on the first story reached its positive maximum strength of 148.0 kN. The split failure occurred at the base of column immediately afterward, and the reduction in strength led to a decrease of approximately 15% in the shear force at the first story. There was no reduction in strength under negative loading conditions. Under the loading was increased up to 1/15 rad, significant cracking occurred at the upper end of the west column (see Photo 8). The loading was applied and then reduced repeatedly, ending with the load applied at a lateral displacement.

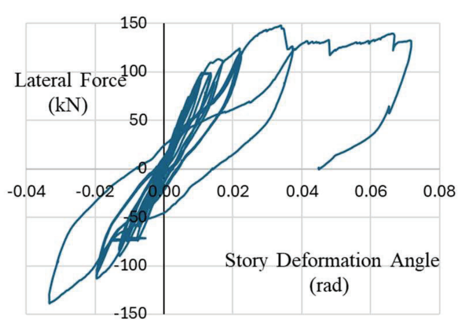

Fig. 24 Lateral Force-Story Deformation Angle Relationship (first story)

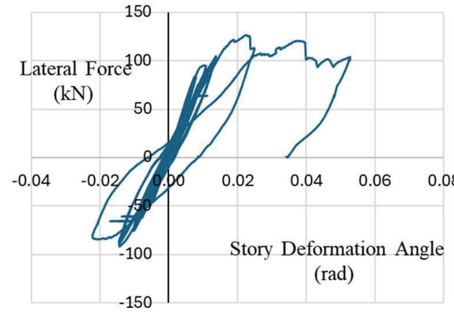

Fig. 25 Lateral Force-Story Deformation Angle Relationship (second story)

Photo 7 Failure modes
+1/15rad East column splitting failure

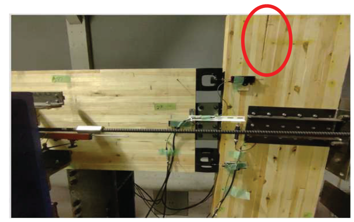

Photo 8 Failure modes
+1/15rad Splits from the west upper shear connecter position

5.2 Characteristic Values

Table 2 presents a list of the characteristic values obtained from the tests. Note that the structural characteristic coefficient was derived based on positive loading up to 1/15 rad and negative loading up to 1/30 rad. The initial stiffness was greater for the first story compared to the second story, both under positive and negative loading conditions. Furthermore, when comparing the positive and negative loading for each story, the stiffness was greater under positive loading for both storys. This is believed to be due to the fact that the joints where the third-floor level jacks were attached in the process of applying the load on the negative side, preventing sufficient load from being applied. When comparing the maximum strength at 1/30 rad for the first and second storys, the positive loading was higher by approximately 10 to 25 kN on both storys.

https://doi.org/10.52202/080513-0019

Table 2: List of characteristic values

	First story		Second story	
	Positive	Negative	Positive	Negative
Initial stiffness K[kN/rad]	11455	8176	5202	4844
Maximum strength Pmax[kN]	148.0	138.7	126.4	91.6
Deformation angle at maximum strength Rmax[$\times 10^{-2}$rad]	2.97 (1/34)	3.29 (1/30)	2.29 (1/44)	1.46 (1/68)
Plasticity ratio μ	3.93	2.01	1.15	1.41
Structural characteristic coefficient Ds	0.38	0.57	0.88	0.81

6 – CONCLUSION

This study develops a joint system using connectors that improve deformation performance and conducts structural experiments assuming the joints of a 3-4 story wooden frame building, along with performance evaluation. Additionally, a full-scale lateral loading experiment was conducted.

Moving forward, a detailed examination will be conducted regarding the consistency between the results of the joint experiments and the full-scale frame tests using this joint system.

REFERENCES

[1] Kenichi Sato et al.: Study on Strength Mechanism of Joint System of Metal Connector and Adhesive in Timber Structures Part.26 Simplify of Calculation Method to Simplify Bending Moment Resisting Performance of Beam-Column Joint, AIJ, Proceedings of the Architectural Institute of Japan Annual Conference, Structure III, pp. 549-550, July 2023. In Japanese

[2] Allowable Stress Design for Wooden Frame Houses (2017 Edition): Japan Housing and Wood Technology Center, March 2017.

[3] Sato, N.; Uetsuki, K.; Tanaka, K.: DEVELOPMENT OF GLULAM COLUMN RC BASE CONNECTION SYSTEM FOR MULTITORIES LARGESCALE TIMBER BUILDING, WCTE 2016 e-book: containing all full papers submitted to the World Conference on Timber Engineering (WCTE 2016), August 22-25, 2016, Vienna, Austria, pp5361-5368

https://doi.org/10.52202/080513-0019